

SPIRAL VIBRATIONS OF ROTORS

J. Schmied
Sulzer Escher Wyss Ltd.
Zurich, Switzerland

ABSTRACT

A method to calculate spiral vibrations of a multi bearing rotor on the basis of the Finite Element method is described. In order to verify the method it is applied to a simple flexible rotor with two concentrated masses. In addition, a practical example of a multi bearing turbine generator is investigated, considering two effects that might cause spiral vibrations: friction in journal bearings and at sliprings.

NOMENCLATURE

c constant added heating efficiency
d diameter
damping coefficient
D modal damping factor
D matrix containing damping and gyroscopic coefficients
f frequency
f vector of the exciting forces
I unit matrix
K stiffness matrix
K_R stiffness matrix of the rotor alone
l length
m mass
m_B mass of a brush
M mass matrix
n rotational speed
number of brushes per circuit
n₁ number of brushes per length
N₁ number of degrees of freedom of the system
p proportionality factor for the added heating efficiency, if it is proportional to the deflection of the shaft
p* proportionality factor for the added heating efficiency, if it is proportional to the radial acceleration of the shaft
P matrix containing the parameter for the added heat
q proportionality factor for the eliminated heating efficiency
Q heating efficiency
Q matrix containing the parameter for the eliminated

heat
s oil film thickness
t time
T period of the spiral to complete 360°
T matrix describing the linear relation between the thermal deflections of all coordinates and the translatory coordinates at the hot spot
T coordinate for translatory deflections
x coordinate for translatory deflections
X vector of all coordinates
X_T vector for the thermal deflections
α real part of the "thermal" eigenvalue
β distribution factor for the added heat
φ coordinate for rotational deflections
ψ circumferential angle
λ "thermal" eigenvalues
ν imaginary part of the "thermal" eigenvalue
μ friction coefficient
θ temperature
ρ radius of a circular orbit
δ_T thermal deflection of a node in direction of its maximum
τ shear stress
Ω angular velocity of the shaft

subscripts

h horizontal direction
v vertical direction
hs location of the hot spot
T thermal deformation

1. INTRODUCTION

Spiral vibrations are often observed in rotors with seal rings, sliprings or journal bearings as well as in connection with shaft rubbing.

In all cases the rotor vibration may induce a hot spot on the surface of the rotor due to friction and cause a thermal bow. Thus the vibration changes and the hot spot and the thermal bow move gradually around the shaft, decreasing or increasing in magnitude. Fig. 1 shows the polar plot of a vibration observed on the bearing of a 600 MVA turbine generator resulting from the described effect.

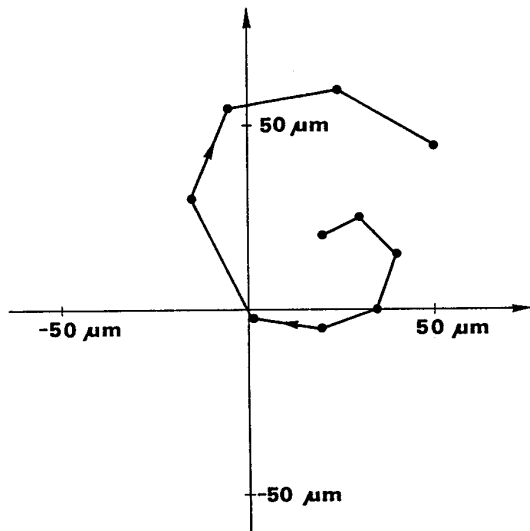


Fig. 1 Polar plot of a measured vibration signal for the case of a spiral vibration.

An increasing spiral must be prevented, either by avoiding components, where hot spots may arise or by making sure that hot spots lead to a decreasing spiral vibration. The latter measure is in many cases the only solution since journal bearings, sliprings and seal rings can not be replaced easily. It requires however the knowledge of the conditions when a spiral increases or decreases.

Spiral vibrations, also called Newkirk effect, have been investigated in the past by A.D. Dimarogonas (1973), W. Kellenberger (1977, 1978, 1979), and other investigators, which are mentioned in the latest paper of W. Kellenberger, where a brief review about earlier investigations is given. W. Kellenberger describes the effect by linear equations whereas A.D. Dimarogonas obtains nonlinear equations. Both authors investigate simple models of rotors.

This paper for the first time deals analytically with a multi bearing turbine generator. The procedure how to consider the thermal effects is based on Kellenberger (1978, 1979). The mechanical equations of motion are extended by a linear thermal equation, which is coupled to the mechanical equations. The necessary extensions in the global matrices of the original Finite Element model of the rotor can be made by using the Finite Element program MADYN (H.D. Klement (1982)), where the user can define values to be added in an arbitrary place in the global matrices of the structure.

The method is verified by applying it to a simple flexible rotor with two masses, which has been investigated earlier by W. Kellenberger (1978).

The following two paragraphs describe how sliprings and journal bearings can cause hot spots.

The effect of these hot spots on a real machine - a multi bearing turbine generator - is studied at the end of this paper by applying the new method.

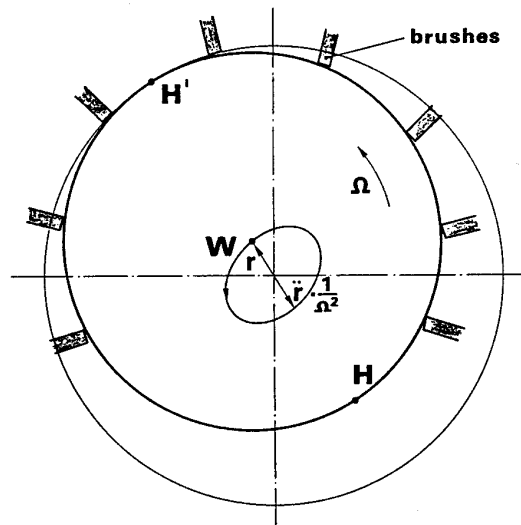


Fig. 2 Orbit of the shaftcenter at the sliprings

2. HOT SPOTS DUE TO SLIPRINGS

Fig. 2 shows the orbit of the center of shaft W at the slipping of a rotor. The brushes are pressed against the surface of the ring by springs, which have the property of causing a pressure not depending on the deflection r of the shaft.

The pressure however may change due to the inertia of the brushes. Brushes in direction of the radial acceleration \ddot{r} of the shaft are pressed by $m_b \ddot{r}$ stronger, those on the opposite side by the same amount weaker against the shaft. Since the orbit and the revolution of the shaft have the same period, the pressure at the point H of the surface is always higher than at the point H'. Thus the friction at H is larger than at H' and a temperature gradient arises from H to H'.

The pressure of the brushes on the shaft may also change due to the friction of the brushes in their holder. This effect however is not considered here.

3. HOT SPOTS DUE TO JOURNAL BEARINGS

Fig. 3 shows very simplified the distribution of the oil film velocity at the two points 1 and 2 of the journal for two positions of the center of the journal. The dashed lines show the situation if the center of the journal has its static position W_0 for a certain rotational speed whereas the solid lines show the situation if the center of the journal is in the point W of its orbit.

Compared to the situation in W_0 the gradient of the velocity of the oil film on the surface of the journal increases in point 1 and decreases in point 2. This causes a higher friction in point 1 and a lower friction in point 2 compared to the static position, because the shear stress is proportional to the gradient of the velocity. Since the orbit of the center of the journal and the revolution of the shaft have the same period, the friction in point 1 is always higher and the friction in point 2 always lower compared to the frictions in the static position. Thus a temperature gradient arises from point 1 to 2.

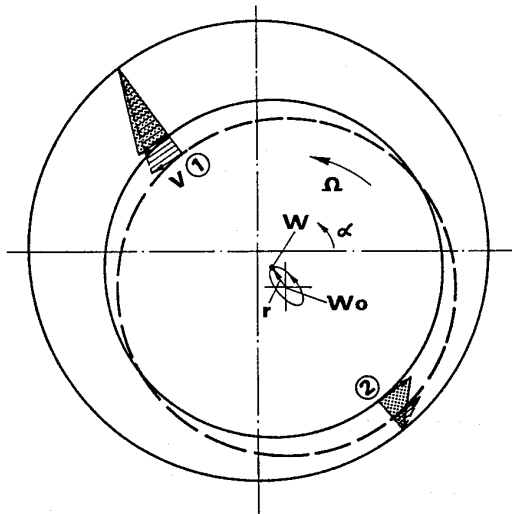


Fig. 3 Profiles of the oilfilm velocities at two points of the journal.

4. COMPUTATIONAL APPROACH

The equation of motion of the Finite Element model of a multi bearing turbine generator has the form

$$M\ddot{x} + D\dot{x} + Kx = f(t) \quad (1)$$

where M is the mass matrix
 D is the matrix containing damping and gyroscopic coefficients and
 K is the stiffness matrix.
 K and D are non symmetric, since they contain the damping and stiffness coefficients of the journal bearings.
 If the rotor is thermally deformed the equation of motion for coordinates x relative to the static position of the undeformed rotor is

$$M\ddot{x} + D\dot{x} + Kx - K^R x_T = f(t) \quad (2)$$

where K^R is the stiffness matrix of the rotor alone (without pedestals and journal bearings) and x_T is the vector describing the thermal deformation.

We assume that the coordinates of the thermal deformation x_T linearly depend on the thermal deflections x_{Ths} of the shaft at the location of the hot spot, that is

$$x_T = I x_{Ths} \quad (3)$$

$$x_{Ths} = (x_{Th}, x_{Tv})^T \quad (4)$$

where x_{Th} and x_{Tv} are the thermal translatory deflections in horizontal and vertical direction at the location of the hot spot. The matrix I is derived from the thermal deformation of the rotor, which is determined by a static calculation with thermal loads, that is a temperature gradient in horizontal direction for the first column of I and a temperature gradient in vertical direction for the second column.

The change of the thermal deflection is described by the following equation

$$\dot{x}_{Ths} = \underbrace{p}_{\dot{Q}^+} \Omega \tilde{x}_{hs} - \underbrace{q}_{\dot{Q}^-} \tilde{x}_{Ths} \quad (5)$$

where $\tilde{x}_{hs} = (\tilde{x}_h, \tilde{x}_v)^T$ is the vector of the translatory shaft deflections at the location of the hot spot,
 \dot{Q}^+ is the added heating efficiency and
 \dot{Q}^- is the eliminated heating efficiency.

Equation (5) has been deduced in detail by Kellenberger (1978 and 1979). The coordinates in (5) are rotating in contrast to the coordinates in (1), (2) and (3), which are stationary.

In (5) the added heat is proportional to the deflection of the shaft at the location of the hot spot. This is a good approximation for the effect in the journal bearing. In case of the effect at the sliprings however, the added heat is proportional to the radial acceleration of the shaft at the location of the hot spot. For a stationary vibration we may write for the radial acceleration

$$\ddot{\tilde{x}}_{hs} = -\Omega^2 \tilde{x}_{hs} \quad (6)$$

For a spiral vibration, which is not stationary, we also assume (6), since the changes are very slow.

Introducing a new proportionality factor p^* for this case

$$p = -p^* \Omega^2 \quad (7)$$

equation (5) may be written as follows:

$$\dot{x}_{Ths} = -p^* \Omega^3 \tilde{x}_{hs} - q \tilde{x}_{Ths} \quad (8)$$

Transforming equation (5) into stationary coordinates x_{Th}, x_{Tv}, x_h, x_v yields

$$\begin{bmatrix} 1 & 0 \\ 0 & 1 \end{bmatrix} \begin{bmatrix} \dot{x}_{Th} \\ \dot{x}_{Tv} \end{bmatrix} + \begin{bmatrix} -p\Omega & 0 \\ 0 & -p\Omega \end{bmatrix} \begin{bmatrix} x_h \\ x_v \end{bmatrix} + \begin{bmatrix} q & \Omega \\ -\Omega & q \end{bmatrix} \begin{bmatrix} x_{Th} \\ x_{Tv} \end{bmatrix} = \begin{bmatrix} 0 \\ 0 \end{bmatrix} \quad (9)$$

or by using matrices and vectors

$$I \dot{x}_{Ths} + P x_{hs} + Q x_{Ths} = 0 \quad (10)$$

Substituting (3) into (2) and extending (2) by (10) yields

$$\begin{bmatrix} M & 0 \\ 0 & 0 \end{bmatrix} \begin{bmatrix} \ddot{x} \\ \dot{x}_{Ths} \end{bmatrix} + \begin{bmatrix} D & 0 \\ 0 & I \end{bmatrix} \begin{bmatrix} \dot{x} \\ \dot{x}_{Ths} \end{bmatrix} + \begin{bmatrix} K & -K^R I \\ \bar{P} & Q \end{bmatrix} \begin{bmatrix} x \\ x_{Ths} \end{bmatrix} = \begin{bmatrix} f(t) \\ 0 \end{bmatrix} \quad (11)$$

where \bar{P} is a $2 \times N$ matrix (with N as the dimension of (2)), which has the coefficients of P at the columns of the translatory coordinates x_{hs} of the hot spot.

In case we use equation (8) instead of (5) p must be substituted by $-p^* \Omega^2$.

To calculate spiral vibrations the original Finite Element model of the rotor represented by equation (1)

must be extended by introducing the two extra degrees of freedom x_{Th} and x_{Tv} . The additional coefficients must be added to the global matrices. This possibility is provided for the input of the program MADYN (H.D. Klement (1982)).

From equation (11) one could calculate the time history of x by a time step method. The polar plot of the time history of each coordinate would be a spiral either increasing or decreasing in magnitude. This calculation however would require a great computational effort, since the period of a spiral to complete 360° is very long for realistic examples. That is why the computation would have to be done for quite a long period of time until one could tell whether a spiral increases or decreases in magnitude.

This information however can also be extracted from the eigenvalues of equation (11). Their calculation requires much less computational effort. The program MADYN provides two methods to determine complex eigenvalues: The Hessenberg method and an inverse vector iteration.

Equation (11) has $2(N+1)$ eigenvalues. Since realistic values for p and q are very small - p is in the order of magnitude of 10^{-4} and q is in the range of $10^{-3} \omega_0$ where ω_0 is a representative natural frequency of the structure (see Kellenberger (1978)) - a set of $2N$ eigenvalues are practically the same as those of equation (1) representing the structure. The additional two eigenvalues are a conjugate complex pair

$$\lambda = \alpha \pm i\nu \quad (12)$$

which is called thermal eigenvalue in the following.

The imaginary part ν of this eigenvalue is almost equal to Ω . This can be explained mathematically by the thermal equation (9). For $p = 0$ this equation is decoupled from the structural equation and has the eigenvalues $\lambda = -q \pm i\Omega$. For $p \neq 0$ the eigenvalue changes due to the coupling to the structure. The change of the imaginary part is only small, since p is very small, hence the coupling is weak.

The change of the real part however is substantial, because q is also very small.

It is obvious that the thermal eigenvalue must have an imaginary part almost equal to Ω , since a constant thermal bow of the shaft rotates with Ω in a stationary coordinate system. The bow however moves gradually around the shaft. That is why ν is slightly different from Ω .

The difference between ν and Ω tells us how fast the bow moves around the shaft respectively at which speed the spiral is traced. The period to complete 360° is

$$T = 2\pi / |\nu - \Omega| \quad (13)$$

The direction of the revolution is as follows:

- $\nu > \Omega$ same direction
- $\nu < \Omega$ opposite direction of the rotor's revolution.

The real part α of the thermal eigenvalue λ tells us whether the spiral increases or decreases in magnitude:

$$\begin{aligned} \alpha > 0, & \text{ increasing magnitude} \\ \alpha < 0, & \text{ decreasing magnitude} \end{aligned} \quad (14)$$

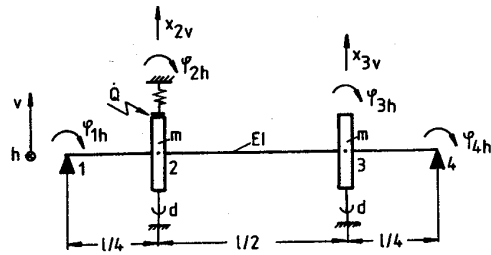


Fig. 4 Model of a simple rotor

5. A SIMPLE EXAMPLE

In order to verify the method described in the previous paragraph, it is applied to the rotor in fig. 4. The rotor has a flexible, massless shaft and two disks of the mass m . It is assumed that the disks do not have any moments of inertia. The translatory movements of the disks are damped by two dampers in horizontal and vertical direction at each disc. The heat is added at the left mass. The added heat is proportional to the deflection of this mass as indicated by the spring. W. Kellenberger (1978) has derived an approximate, analytical solution of the spiral vibration of the translatory coordinates of node 2 of this model. This solution can serve as comparison with the solution according to our method.

We model the stiffness property of the rotor by massless beam elements. The coordinates of the model for the vertical bending direction are shown in fig. 4.

The assumed shape for the thermal deformation due to a hot spot at node 2 is shown in fig. 5. This shape corresponds to Kellenberger's assumption, that the thermal deflection of the right mass is one third of the thermal deflection of the left mass.

If the thermal deformation in fig. 5 is in vertical direction, it can be described by the following vector:

$$\begin{pmatrix} \psi_{1v} & x_{2h} & \psi_{2v} & x_{3h} & \psi_{3v} & \psi_{4v} \end{pmatrix} = \begin{pmatrix} -4/1 & 1 & -4/(3l) & 1/3 & 4/(3l) & 4/(3l) \end{pmatrix}^T \quad (15)$$

The same shape in horizontal direction can be described in the same way with the corresponding coordinates. The elements of the vector in (15) are used in the matrix \underline{I} (see equation (3)).

In the following, the frequency

$$\omega_0 = \sqrt{216 EI / (l^3 m)} \quad (16)$$

is used as a reference frequency as by Kellenberger.

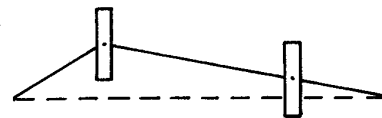


Fig. 5 Assumed thermal deformation

The first two eigenfrequencies of the undamped system without hot spot are

$$\omega_1 = 0.471 \omega_0, \quad \omega_2 = 1.333 \omega_0 \quad (17)$$

For the damping coefficient d and the proportionality factor q , the following fixed values are chosen as by Kellenberger:

$$d = 0.1 m \omega_0 \quad (18)$$

$$q = 10^{-3} \omega_0 \quad (19)$$

The proportionality factor p and the angular velocity Ω are varied. The following examples are calculated:

- 1) $\Omega = 0.4 \omega_0, \quad p = 1.15 \cdot 10^{-3}$
- 2) $\Omega = 0.4 \omega_0, \quad p = 1.235 \cdot 10^{-3}$
- 3) $\Omega = 1.2 \omega_0, \quad p = 0.57 \cdot 10^{-3}$
- 4) $\Omega = 1.2 \omega_0, \quad p = 0.59 \cdot 10^{-3}$

Table 1 shows the calculated thermal eigenvalues and the period T according to equation (13) for the spiral to complete 360° . The period T in hours is calculated by means of $n_s = \omega_s / 2\pi$, where n_s has the dimension 1/min., as follows:

$$T = \frac{1}{|\Omega/\omega_0 - \nu/\omega_0| n_s} \quad (20)$$

Table 1: Thermal eigenvalues of the calculated examples and period T , $n_s = 1000$ 1/min

Example	$\alpha/\omega_0 \cdot 10^5$	ν/ω_0	T [h]
1	-5.7339	0.39950	0.033
2	1.1499	0.39947	0.031
3	-1.6850	1.19961	0.043
4	1.7338	1.19960	0.042

The values for T , the direction of the spiral's revolution and the stability coincide with Kellenberger's results. The direction of the spirals' revolution is always against the rotor's revolution, since the values for ν/ω_s are smaller than the rotational speed Ω/ω_s . The stability is assessed by the sign of α/ω_s .

6. ESTIMATING THE PROPORTIONALITY FACTORS p , p^* AND q

In the previous paragraph, the same values as by Kellenberger were chosen for the proportionality factors p and q . He estimated the values by comparing the calculated results with observations in real machines.

In the following we try to derive approximate formulas to calculate p , p^* and q from the physical effects described in paragraph 2 and 3, in order to find out later (see paragraph 7), if these effects can be responsible for the observed spiral vibrations in the investigated real machine.

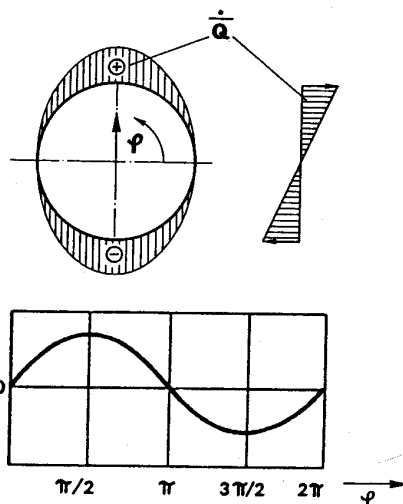


Fig. 6 Circumferential distribution of the added and eliminated heating efficiency

For this purpose the term representing the added heat in equation (5) respectively (8) is assumed to be constant. This assumption can be made, because the change of the vibration of the rotor is very slow and because the change of the added heat during one revolution of the rotor can be neglected, since the thermal time constants are much larger than the period of the rotor's revolution.

With this simplification equation (5) respectively (8) may be written as follows

$$\dot{\rho}_T = c - q \rho_T \quad (21)$$

with ρ_T as the thermal deflection at the location of the hot spot in direction of its maximum.

With the initial condition $\rho_T(0) = 0$ (21) has the solution

$$\rho_T = c/q (1 - e^{-qt}) \quad (22)$$

This function may be adapted to the time history of the thermal deflection resulting from a calculation or measurement, when the shaft is heated constantly at the location of the hot spot with a circumferential distribution of the added and eliminated heat efficiency according to fig. 6, which shows the difference to the mean added heating efficiency.

The adaption can be done at two instants. From the stationary thermal deflection $\rho_T(t=\infty)$ follows from (22)

$$c = q \rho_T(t=\infty) \quad (23)$$

From an arbitrary instant t_1 follows from (22) by using c according to (23)

$$q = -1/t_1 \ln(1 - \rho_{T1}/\rho_{T\infty}) \quad (24)$$

Equation (24) directly yields the parameter q , whereas the parameter p , respectively p^* must be extracted from c . For this purpose we assume that the orbit of the

center of the shaft is a circle with the radius ρ . In this case we may write for c

$$c = \rho \Omega \rho \quad (25)$$

respectively

$$c = -\rho^* \Omega^3 \rho \quad (26)$$

From these two equations the proportionality factors may be determined, if the value of the radius is known. It has the value necessary to produce the difference $\Delta \dot{Q}$ of the added and eliminated heating efficiency assumed in the calculation of the time history of the thermal deflection

In case of a hot spot at the sliprings, the relation between $\Delta \dot{Q}$ and ρ is found by calculating the pressure forces of the brushes on the surface of the ring due to the shaft acceleration as a function of Ωt , summing up the difference between positive and negative forces, averaging it for one revolution of the shaft and calculating the power of the friction due to the averaged force difference. Since not all the friction power necessarily enters the shaft as heating efficiency, a distribution factor β is introduced. The thus calculated $\Delta \dot{Q} - \rho$ relation is

$$\rho = \frac{\pi \Delta \dot{Q} / l}{\beta n n_L m_B \Omega^3 \mu d} \quad (27)$$

where $\Delta \dot{Q} / l$ is the difference $\Delta \dot{Q}$ per length, n the number of brushes per circuit, n_L the number of brushes per length, m_B the mass of one brush, μ the friction coefficient, d the diameter of the ring and β the distribution factor.

In case of a hot spot in the bearing, the change of the shear stress $\Delta \tau$ in direction of the deflection ρ , which is equal to the change Δs of the oilfilm thickness s , is approximated by the linear terms of a Taylor extension of the function

$$\tau = c/s \quad (28)$$

where c is a constant. The mean oilfilm thickness for the static position of the journal s_0 is chosen as the reference oilfilm thickness for the extension. The constant c can be determined from the known power loss P in the bearing. Assuming a circumferential distribution of $\Delta \tau$ according to \dot{Q} in fig. 6, calculating the difference between the positive and negative power due to $\Delta \tau$ by integration and again introducing a distribution factor β yields the following relation

$$\rho = \frac{\pi \Delta \dot{Q}}{2 P_L \beta} s_0 \quad (29)$$

7. A PRACTICAL EXAMPLE

Fig. 7 shows the rotor investigated in the following consisting of a high pressure, an intermediate pressure, two low pressures, a generator and a rotor for the sliprings. The whole rotor has nine bearings and a total length of 41.8 m. The external support consisting of pedestals and foundation is modelled by a mass and two springs in horizontal and vertical direction.

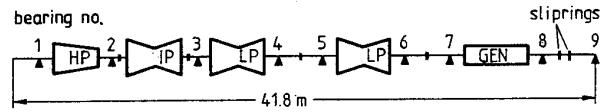


Fig. 7 Model of the real machine

The rotor was very critical to problems with spiral vibrations in the area of the slipring rotor. The machine was very carefully checked with regard to any rubbing of the rotor at the housing, so that this can be ruled out as the reason for the trouble. The seal rings also did not clamp. Remaining causes for the problem could be hot spots in the bearing number 8 and at the sliprings.

Fig. 8 and fig. 9 show the thermal deformation of the rotor for a constant temperature gradient of $\Delta T = 1^\circ\text{C}$ over the rotor diameter at the sliprings and in the journal of bearing number 8. In both cases we have large thermal deformations in the slipring rotor, which is a certain explanation for the trouble in this part of the rotor.

In case of the hot spots at the sliprings, we have two points where heat is added to the shaft. The method of calculation in paragraph 4 is described for just one hot spot. Although the method could easily be extended to more hot spots, we assume that the heat is added at just one point (between the sliprings). This is just a minor simplification, since the two sliprings are quite close.

Fig. 10 and 11 show the stability chart for the two cases. The threshold was determined by searching the required p respectively p^* for a certain q to fulfil the condition $\alpha = 0$, with α as the real part of the thermal eigenvalues (see equation (12)). This was done by linear interpolation from two real parts α for two different pairs of values of p respectively p^* and q . The stability threshold determined in this way is exact within the limits of the theory, since α linearly depends on p and q as was found out by a number of calculations.

The areas of instability, that is the areas where the spiral increases, are very similar for the two cases. Below the critical speed of the vertical mode of the slipring rotor (mode 15 in fig. 12) no instability can occur. Above this critical speed also at the nominal speed of 50 1/s instabilities are possible. Other

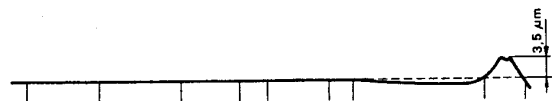


Fig. 8 Thermal deformation of the rotor for hot spots at the sliprings $\Delta T = 1^\circ\text{C}$

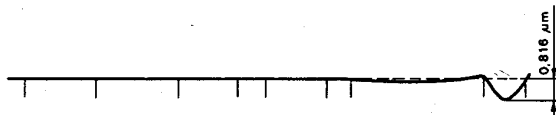


Fig. 9 Thermal deformations of the rotor for a hot spot in the bearing no. 8, $\Delta T = 1^\circ\text{C}$

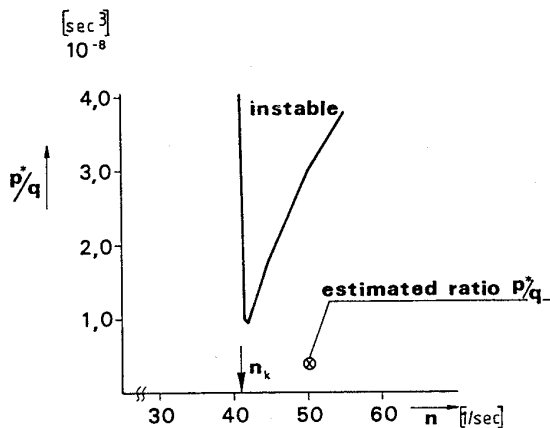


Fig. 10 Stability chart for the hot spots at the sliprings

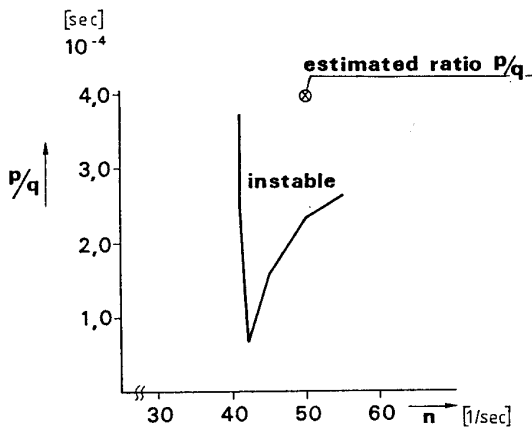


Fig. 11 Stability chart for the hot spot in bearing no. 8

critical speeds present in this area do not interfere, in spite of considerable deflections of the mode shapes in the slipping rotor.

To judge, whether the demonstrated instability areas may be responsible for the trouble with spiral vibrations, values of p , p^* and q are estimated according to the method described in paragraph 6.

The thus determined values however are just a very rough estimation, since the method is just an approximation and some parameters like the distribution factor and the friction factor (see equation (27) and (29)) are very uncertain. Regarding these uncertainties the calculation of the time history of the thermal deflection for constant heating was made quite rough, that is the heat conduction in the shaft in axial direction was neglected. Fig. 13 shows the time history of the maximum deflection calculated in this way for a distribution of the added and eliminated heat in the journal of bearing 8 according to fig. 6. The dashed line shows the adapted curve. It is obvious that one time constant is not enough for an exact adaptation. It is however good enough for a rough estimation.

No.	f [Hz]	D dominating direction	mode shape
12	35.676	0.052 h	
13	35.918	0.011 v	
14	37.671	0.030 h	
15	41.036	0.020 v	

Fig. 12 Natural modes of the rotor between 30 Hz and 50 Hz

The ratios p^*/q and p/q for the estimated values are shown in fig. 10 and 11. It can be seen that p^*/q is not in the instability area, although the maximum value of $\beta = 1$ has been chosen for the distribution factor. The ratio p/q however is in the instability area if the value $\beta = 1.0$ is chosen for the distribution factor. It seems that a hot spot in bearing 8 is the major reason for the trouble with spiral vibrations in this machine. A hot spot at the sliprings however may intensify the effect of the hot spot in bearing number 8.

A hint that the trouble is mainly caused in the bearing number 8 is also the fact that in practice the behavior of the spiral vibration was very sensitive to changes of the oil temperature and oil flow.

The machine was readjusted by taking measures to reduce the eigenfrequency of the vertical mode of the slipping rotor. This had the effect of shifting the instability areas to the left (see fig. 10 and 11). The machine ran well after this.

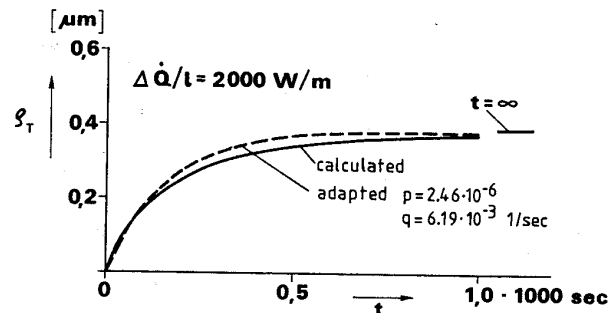


Fig. 13 Time history of the thermal deflection of the shaft at bearing no. 8

8. CONCLUSIONS

A method to calculate spiral vibrations of a multi bearing generator rotor with the Finite Element Program MADYN was described. In order to check the method, some results of a simple flexible rotor with two masses were calculated. The results were compared with those of W. Kellenberger, who has investigated this model before. The coincidence was very good.

The method was also applied to a real machine - a multi bearing turbine generator. Its behavior with regard to hot spots at the journal of a bearing and at the sliprings was studied. A stability chart was determined for both cases, showing the areas with an increasing and decreasing spiral. The critical speed of the vertical mode of the slipring rotor, where the thermal deflections due to the hot spots are large, proved to be essential for the location of the instability areas. By estimating roughly the thermal parameters, it was concluded that those instability areas could be responsible for the sensitivity of this machine concerning spiral vibrations. The measures to readjust the machine deduced from the results were successful.

ACKNOWLEDGEMENT

The investigations for this paper were done at the Brown Boveri Company in Baden, Switzerland. The author wishes to thank the company for the support granted to him, which made this work possible.

REFERENCES

- Dimarogonas, A.D., 1973
"Newkirk Effect, Thermally Induced Dynamic Instability of High Speed Rotors", International Gas Turbine Conference, Washington D.C., April 1973, ASME-Paper No. 73-GT-26.
- Kellenberger, W., 1977
"Quasi-stationäre Schwingungen einer rotierenden Welle, die an einem Hindernis streift - Spiral Vibration."
Ingenieurarchiv 46 (1977) 349 - 364.
- Kellenberger, W., 1978
"Das Streifen einer rotierenden Welle an einem federnden Hindernis - Spiralschwingungen."
Ingenieurarchiv 47 (1978) 223 - 229.
- Kellenberger, W., 1979
"Spiral Vibrations Due to the Seal Rings in Turbogenerators Thermically Induced Interaction between Rotor and Stator".
Design Engineering Conference, St. Louis, Sept. 78, ASME-Paper No. 79-DET-61.
- Klement, H.D., 1982
"Eingabebeschreibung MADYN". Fachgebiet Maschinendynamik TH-Darmstadt.

reprinted from

Rotating Machinery Dynamics Volume Two - DE-Vol. 2
Editors: A. Muszynska, and J.C. Simonis
(Book No. H0400B)

published by

THE AMERICAN SOCIETY OF MECHANICAL ENGINEERS
345 East 47th Street, New York, N.Y. 10017
Printed in U.S.A.